STREAK CAMERA CALIBRATION USING RF SWITCHES

U. Iriso, M. Alvarez, A.A. Nosych, ALBA-CELLS, Barcelona, Spain
A. Molas, Universitat Autónoma de Barcelona, Spain

Abstract

The streak camera has been used to measure the bunch length since the ALBA storage ring commissioning in 2011. Previously, we developed an optical calibration system based on the Michelson interferometry. In this report, we show the electronic calibration system based on the work in DLS [1], and compare both calibration systems. Finally, we show measurements of the longitudinal impedance obtained with the new calibration.

INTRODUCTION

ALBA is equipped with a beam diagnostics beamline (BL34- Xanadu) that uses the visible part of the synchrotron radiation to characterize both longitudinal and transversely the electron beam profile [2, 3]. In the longitudinal plane, the key instrumentation is the Streak Camera (SC), which allows precise bunch length measurements and longitudinal beam dynamics studies. The camera is the Optronis SC-10 model, with a synchroscan frequency working at 250 MHz to distinguish the beam bunches spaced by 2 ns [4].

In order to perform precise measurements using the streak camera, it is necessary to determine the calibration factor that provides the relationship between the number of pixels and the corresponding time units. Moreover, Ref. [2] shows that depending on the speed sweep unit of the streak camera, this calibration might not be completely linear and a multi-linear calibration is required. This is especially the case for the slowest synchroscan speed of 50 ps/mm, while the speeds of 25 and 15 ps/mm show a very linear behaviour.

At ALBA, this factor was calibrated in 2012 using an optical set-up based on the Michelson interferometry [2]. The goal in those experiments was to include an optical delay of a known amount in the path of the synchrotron radiation, and measure it using the streak camera. This solution faces two main limitations: on one side, it is not easy to assemble the calibration setup (proper alignment of the optical systems); and secondly, it only provides calibration in the fast (in our case, vertical) sweep speeds.

Instead, the solution developed at Diamond Light Source [1] is based on delaying the reference RF signal used for the fast sweep unit with respect to the synchrotron radiation. This is achieved using RF switches, which change the path length of the RF signal by a known amount. Moreover, since the switching frequency is also known, a calibration pattern for the slow (in our case, hor) scale is also given.

ELECTRONIC CALIBRATION KIT

The layout of the calibration kit is shown in Fig. 1. The $f_{rf}/2$=250 MHz reference signal is introduced in the crate, where two RF switches alternate the signal path between

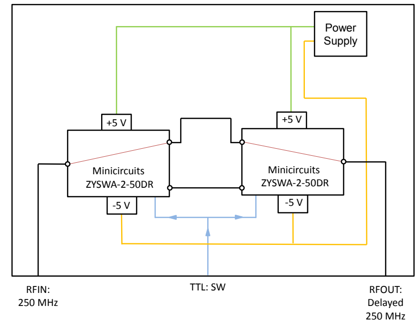

Figure 1: Schematic illustration of the crate used in order to introduce a delay in the 250MHz signal using the PIN diodes switching with a frequency set by the TTL signal and two cables with a certain different length.

a longer or a shorter way, whose difference is called $\Delta\tau$. By precisely measuring the difference in the path length, we can calibrate the streak camera. The RF switches are triggered by an Event Receiver producing TTL square waves, whose switching frequency f_{sw} can be changed at will. The calibration process is disabled if we disable the output on the Event Receiver.

The image obtained in the SC when the calibration kit is in use has the zigzag shape shown in Fig. 2. The image has a symmetry top/bottom, since the SC sends odd bunches to the top half of the image, and bottom bunches to the bottom.

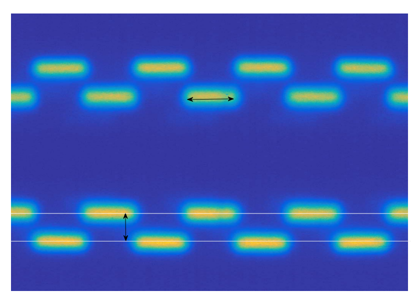

Figure 2: Output image of the streak camera after performing the delay of the 250MHz signal with the RF switches.

Note that:

- The horizontal scale is calibrated using the distance between streaks, which corresponds to $0.5/f_{sw}$ (see horizontal arrow in Fig. 2).
- The vertical scale is calibrated using the distance between the zigzag streaks, which corresponds to the time delay given by the cable difference, $\Delta\tau$ (see vertical arrow in Fig. 2).

ISBN 978-3-95450-177-9

Delay Characterization

We use the VNA Agilent E5071B (300 kHz – 8.5 GHz) to measure the time difference between the cables in Fig. 1. The measurement is performed from the phase difference measured on a 250 MHz signal with the RF switches on. An example of this measurement is shown in Fig.3 for a switching frequency of 10 Hz. The measured delay between cables is (77.298 ± 0.015) ps.

The delay between the cables are measured using different switching frequencies, spanning from 10 Hz to 4 kHz. The variation of the length difference changes only by ~ 0.5%, so we conclude that the average value of the delay is:
$\Delta\tau$ **= 77.420** ± **0.080 ps**.

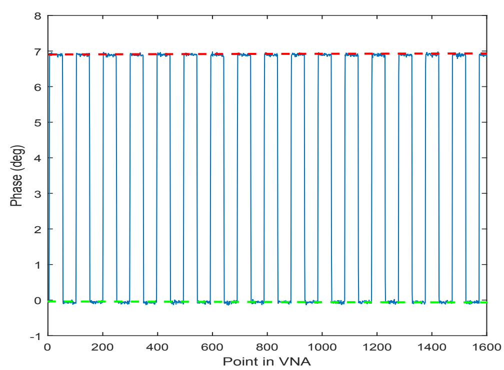

Figure 3: Phase delay between the long and short cables for a 10 Hz switching frequency.

CALIBRATION RESULTS

Horizontal (Slow) Time Unit

The horizontal calibration for the different sweeps speeds of the deflection unit are listed in Table 1. In general, the theoretical factor is always smaller than the measured one by about 10%. The sweep speed in the horizontal time unit is constant and so it is properly characterized by a simple linear factor. (This is not the case for the slowest sweep speeds in the vertical deflection – see next).

Table 1: Horizontal Calibration Factor Measured for Different (Not All) hor Sweep Speeds of the SC

Sweep Speed	Cal. Factor, $\frac{\mu s}{pix}$	Theo. Factor, $\frac{\mu s}{pix}$
5 ms/mm	75.0 ± 0.5	70
1 ms/mm	15.6 ± 0.2	14
500 μs/mm	7.56 ± 0.15	7
100 μs/mm	1.60 ± 0.04	1.4
50 μs/mm	0.790 ± 0.02	0.7
10 μs/mm	0.163 ± 0.005	0.14
5 μs/mm	$(76.8 \pm 1.8)\times10^{-3}$	70×10^{-3}
1 μs/mm	$(16.2 \pm 0.6)\times10^{-3}$	14×10^{-3}
250 ns/mm	$(3.8 \pm 0.1)\times10^{-3}$	3.5×10^{-3}

Vertical (Fast) Time Unite

Since the signal at the vertical deflection unit is sinusoidal, the relation between the pixel position and time is only linear near the center. While the linear approximation for the faster vertical sweep speeds is valid, for the slowest speed (50 ps/mm) the calibration needs to take into account the non-linear effects. For this reason, a piecewise linear aproximation (or *multi-linear* calibration) is used. Since most of our measurements are done using the 50 ps/mm speed, in the following we focus our results on this case.

Figure 4 plots the pixel vs time for different horizontal sweep speeds of the SC. Identical curves are found for sweep speeds between 5 ms/mm to 5μs/mm. On the other hand, the calibration curve using the optical delay described in Ref. [2] is slightly different. While the systematic errors related to the optical system set-up are difficult to evaluate, the errors associated to the calibration kit are below 0.5%.

In the following, the measurements are performed using the results provided by the rf switches calibration kit, considering only a single multi-linear calibration for all horizontal sweep speeds.

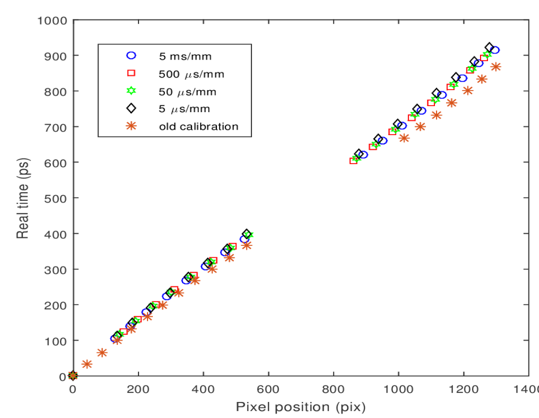

Figure 4: Multilinear calibration for different sweep speeds and using the old calibration from the Michelson interferometry [2]. For the sweep speeds from 5ms/mm to 5μs/mm the multilinear calibration is almost identical.

RECOVERING AN RF PLANT

When one of the 6 RF cavities at ALBA trips, the available voltage decreases and the phase in the rest of the 5 cavities decreases to provide the beam with the necessary energy per turn. This is translated with an increase of the bunch length σ and a shift of the beam centroid ϕ. An example of this case is shown in Fig. 5, which shows the centroid and bunch length evolution during the recovery of an rf cavity. In total, the voltage changes from 2.25 MV to 2.6 MV.

The top plot in Fig. 5 shows the evolution of the difference in the bunch centroid for odd and even bunches as measured in the SC. From the average of this centroid difference, we infer a phase change of $\Delta\phi^{SC} = (3.2 \pm 0.20)°$. On the other hand, the phase measured from the rf power is $\Delta\phi^{RF} = (3.76 \pm 0.60)°$ – see Ref. [5]. Although the results differ by

ISBN 978-3-95450-177-9

~15%, we can conclude the results are consistent if we take into account the associated error bars.

The evolution of the bunch length is shown in Fig. 5 (bottom plot). When the rf cavity is recovered, the bunch length ratio σ_2/σ_1 follows:

$$\frac{\sigma_2}{\sigma_1} = \sqrt{\frac{V_1 \cos\phi_1}{V_2 \cos\phi_2}} \; . \tag{1}$$

While the bunch length ratio is σ_2/σ_1=1.08±0.01, the voltage ratio (rhs of Eq. 1) is 1.092 ± 0.005 corresponding to a disagreement around 1%, from where we conclude that the results are very consistent and the calibration is very good.

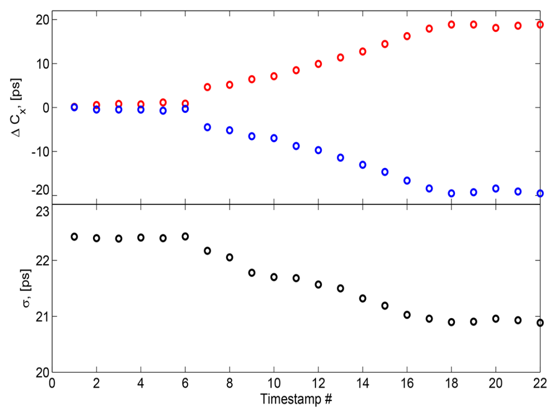

Figure 5: Centroid position (top) and bunch length (bottom) evolution during an RF cavity recovery. The RF voltage goes from 2.3 MV to 2.6 MV in about 5 min, and each timestamp corresponds to approximately 14 sec.

LONG. IMPEDANCE MEASUREMENTS

In order to characterize the ALBA longitudinal impedance, single bunch measurements are carried out at two different voltages, V_0=2.6 MV and V_0=2.35 MV.

Bunch Length Measurements

The longitudinal impedance $\mathrm{Im}(Z_0^{\parallel}/n)_{\mathrm{eff}}$ is determined by measuring the variation in the bunch length σ with single bunch current I_B. Away from the MW-instability, the bunch length parametrisation is:

$$\left(\frac{\sigma}{\sigma_0}\right)^3 - \left(\frac{\sigma}{\sigma_0}\right) = \frac{\alpha_c \mathrm{Im}(Z_0^{\parallel}/n)_{\mathrm{eff}}}{\sqrt{2\pi}(E/e)Q_{s0}^2(\omega_0\sigma_0)^3} \cdot I_B \; , \tag{2}$$

where α_c is the momentum compaction factor, σ_0 is the bunch length in the limit $I_B = 0$, E/e is the beam energy (in eV), and Q_{s0} is the synchrotron frequency.

The bunch profile for different intensities are shown in Fig. 6. Although the profile for low currents is well approximated by a Gaussian shape, the bunch starts to deform with increasing currents. In order to infer the proper value of the bunch length σ, one should solve the so-called Haissinsky equation [6]. This process is currently on-going, and therefore we cannot show exact results of $\mathrm{Im}(Z_0^{\parallel}/n)_{\mathrm{eff}}$.

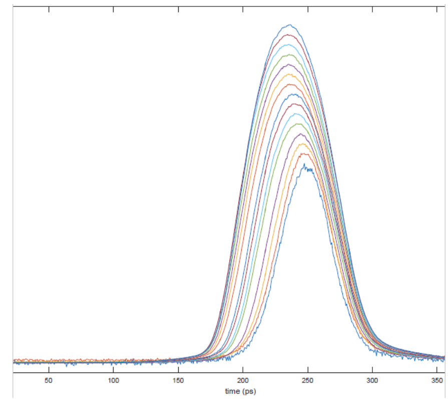

Figure 6: Mountain range plot while increasing the bunch intensity from 0.5 mA (lower trace) to 8 mA (top).

For illustrative purposes, we infer the bunch length σ just by fitting a Gaussian shape to the profiles shown in Fig. 6. This is shown in Fig. 7, where the bunch length increases with increasing current approximately with a I_B dependence. The injection was stopped at 8 mA for safety purposes.

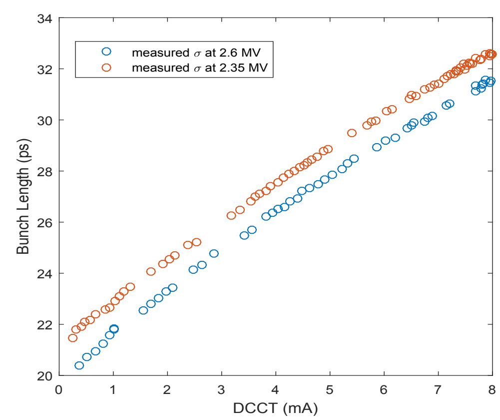

Figure 7: Change of the bunch length during the injection in single bunch mode. The profiles in Fig. 6 are fitted to a simple Gaussian curve.

Centroid Measurements

The loss factor $k_{\parallel}$ of a storage ring relates the energy transfer ΔE per revolution from the beam bunch to the machine vacuum chamber as:

$$\Delta E = k_{\parallel} \cdot Q_B^2 \; , \tag{3}$$

where Q_b is the beam bunch charge. When the beam bunch transfers this energy to the machine, it needs to ride higher on the rf wave to recover this loss and the synchrotron phase ϕ_s shifts. In time domain, the phase shift is expressed as [7]:

$$\Delta T_C = \frac{T_{\mathrm{rf}}}{2\pi} \frac{k_{\parallel} T_0}{V_0 \cos\phi_s} I_B \; , \tag{4}$$

where $T_{\mathrm{rf}} = 1/f_{\mathrm{rf}}$ is the rf period and T_0 is the revolution period. Thus, the loss factor $k_{\parallel}$ is inferred by measuring the

ISBN 978-3-95450-177-9

Table 2: ALBA Parameters and Results during Single Bunch Measurements

mom. comp. factor, α_c	0.0088	
revolution period, T_0[ns]	896	
rf frequency, f_{rf}[MHz]	499.649	
energy, E[GeV]	2.987	
rf voltage, V_0[MV]	2.6	2.35
sync. phase, ϕ_s[°]	152.9	154.2
sync. tune,	0.0071	0.0066
bunch length, σ_0[ps]	18.75	20.26
loss factor, $k_{\parallel}$[V/pc]	14.1± 0.4	13.12 ±0.05
resistance, R[Ω]	935 ± 25	940 ± 5
Re($Z_0^{\parallel}/n$) [mΩ]	127±4	136±1

centroid displacement with respect to the single bunch intensity, which is shown in Fig. 8 for two different rf voltages, 2.35 and 2.6 MV. From the fit in Fig. 8 and using the measured values shown in Table 2, the loss factor is inferred as $k_{\parallel}$ = 14.2 ± 0.4 (for 2.6 MV), and $k_{\parallel}$ = 13.12 ± 0.03 V/pC (for 2.35 MV).

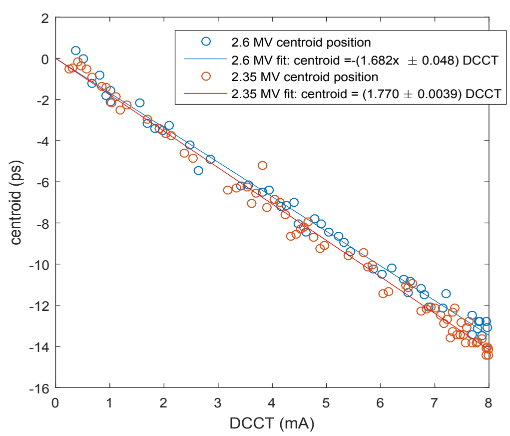

Figure 8: Centroid displacement during an injection in single bunch mode for V_0=2.5 MV and V_0=2.35 MV.

The complete expression of the loss factor for Gaussian bunches is given by:

$$k_{\parallel} = \frac{1}{2\pi}\int_{-\infty}^{+\infty} \mathrm{Re}\, Z_0^{\parallel}(\omega)\cdot e^{-(\sigma\omega)^2}\, d\omega, \tag{5}$$

where $Z_0^{\parallel}$ is the longitudinal impedance, σ is the temporal bunch length and ω is the angular frequency. If one approximates the impedance by a constant resistance R, the loss factor can be simplified by:

$$k_{\parallel} = \frac{R}{2\sqrt{\pi}\sigma_0}, \tag{6}$$

With this assumption, the resistance of ALBA is R=935±25 Ω (2.6 MV), and 940±5 Ω (2.35 MV), which is consistent with values found in other machines [7, 8]. Furthermore, we can approximate:

$$\mathrm{Re}\left(Z_0^{\parallel}\right)_{\mathrm{eff}} \approx R\cdot(\sigma\omega), \tag{7}$$

which provides a value of $\mathrm{Re}\left(Z_0^{\parallel}\right)_{\mathrm{eff}}$ ~130 mΩ (see Table 2), consistent with the expectations. Again, a more precise way to tackle this calculation is by solving the Haissinsky equation.

CONCLUSIONS

We have implemented a calibration kit for our Streak Camera based on the electrical delay between two different cables, whose length is precisely measured with a VNA. The calibration kit allows almost on-line calibration in both the slow (horizontal) and fast unit (vertical). While the horizontal values are typically ~10% larger than the theoretical ones, in the vertical direction we found most convenient to use the slowest sweep speed (50 ps/mm) with a multi-linear calibration whose spread is very small (~0.5%).

Several machine measurements are presented using the calibration results presented in this report. The bunch length evolution during the recovery of an rf cavity at ALBA showed a good agreement with the expectations. Moreover, longitudinal impedance measurements showed values consistent with other machines, although a more careful analysis of the result is foreseen in the near future.

ACKNOWLEDGEMENTS

The authors would like to thank B. Bravo for useful discussions regarding RF issues and T. Guenzel for guiding the impedance calculations.

REFERENCES

[1] L.M. Bobb, A.F.D. Morgan, G. Rehm, *Streak Camera PSF Optimisation and Dual Sweep Calibration for Sub-ps Bunch Length Measurement*, IBIC'15, Melbourne (Australia), 2015.

[2] U. Iriso and F. Fernández, *Streak Camera Measurements at ALBA: Bunch Length and Energy Matching*, IBIC'12, Tsukuba (Japan), 2012.

[3] L. Torino and U. Iriso, *Limitations and Solutions of Beam Size Measurements via Interferometry at ALBA*, IBIC'15, Melbourne (Australia), 2015.

[4] Optronis GmbH, `http://www.optronis.com`

[5] B. Bravo et al, *Calibration of the acceleration voltage of six normal conducting cavities at ALBA*, Proc. of IPAC15.

[6] J. Haissinski, Nuovo Cimento B, 18 (1973).

[7] R.Dowd et al, *Single bunch studies at the Australian Synchrotron*, TUPC010, Proc. of EPAC08.

[8] J.C. Bergstrom, *Jack's Book on Beam Instabilities*, Canadian Light Source Internal Note, 5.17.38.1 (2006)

ISBN 978-3-95450-177-9